Title: A miniaturized electrochemical toxicity biosensor based on graphene oxide quantum dots/carboxylated carbon nanotubes for assessment of priority pollutants

Author: Xiaolin Zhu Guanlan Wu Nan Lu Xing Yuan Baikun Li

PII: S0304-3894(16)30982-7
DOI: http://dx.doi.org/doi:10.1016/j.jhazmat.2016.10.057
Reference: HAZMAT 18138

To appear in: *Journal of Hazardous Materials*

Received date: 10-7-2016
Revised date: 14-10-2016
Accepted date: 24-10-2016

Please cite this article as: Xiaolin Zhu, Guanlan Wu, Nan Lu, Xing Yuan, Baikun Li, A miniaturized electrochemical toxicity biosensor based on graphene oxide quantum dots/carboxylated carbon nanotubes for assessment of priority pollutants, Journal of Hazardous Materials http://dx.doi.org/10.1016/j.jhazmat.2016.10.057

A miniaturized electrochemical toxicity biosensor based on graphene oxide quantum dots/carboxylated carbon nanotubes for assessment of priority pollutants

Xiaolin Zhu[a], Guanlan Wu[a], Nan Lu[a], Xing Yuan[a,*], Baikun Li[b,*]

[a] *School of Environment, Northeast Normal University, Changchun 130117, PR China*

[b] *Department of Civil and Environmental Engineering, University of Connecticut, 261 Glenbrook Road, Unit 2037, CT 06269, USA*

[*] Corresponding author: Tel.+86 431 89165600; Fax: +86 431 89165606
E-mail : yuanx@nenu.edu.cn (X. Yuan)

[*] Corresponding author: Tel. +1 860 486 2339; Fax: +860 486 2298
E-mail: baikun@engr.uconn.edu (B.k. Li)

Graphical abstract

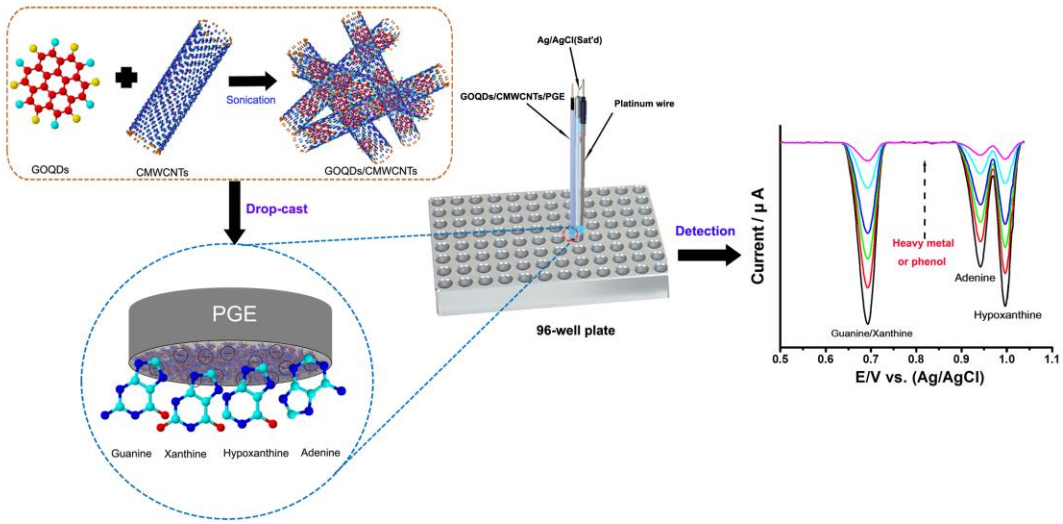

Highlights

- Graphene oxide quantum dots/carboxylated carbon nanotubes hybrid was developed.
- The cytotoxicity detection vessel was miniaturized to the 96-well plate.
- The electrochemical behavior of HepG2 cell was investigated for the first time.
- The mixture signal of adenine and hypoxanthine was separated successfully.
- The biosensor was used to assess the toxicity of heavy metals and phenols.

Abstract

The study presented a sensitive and miniaturized cell-based electrochemical biosensor to assess the toxicity of priority pollutants in the aquatic environment. Human hepatoma (HepG2) cells were used as the biological recognition agent to measure the changes of electrochemical signals and reflect the cell viability. The

graphene oxide quantum dots/carboxylated carbon nanotubes hybrid was developed in a facile and green way. Based on the hybrid composite modified pencil graphite electrode, the cell culture and detection vessel was miniaturized to a 96-well plate instead of the traditional culture dish. In addition, three sensitive electrochemical signals attributed to guanine/xanthine, adenine, and hypoxanthine were detected simultaneously. The biosensor was used to evaluate the toxicity of six priority pollutants, including Cd, Hg, Pb, 2,4-dinitrophenol, 2,4,6-trichlorophenol, and pentachlorophenol. The 24 hr IC_{50} values obtained by the electrochemical biosensor were lower than those of conventional MTT assay, suggesting the enhanced sensitivity of the electrochemical assay towards heavy metals and phenols. This platform enables the label-free and sensitive detection of cell physiological status with multi-parameters and constitutes a promising approach for toxicity detection of pollutants. It makes possible for automatical and high-throughput analysis on nucleotide catabolism, which may be critical for life science and toxicology.

Keywords: Priority pollutants; Cell sensor; Toxicity; Graphene oxide quantum dots; Carbon nanotubes

1. Introduction

Phenols and heavy metals have been included on the priority pollutants list by US Environmental Protection Agency (USEPA) and the European Union (EU) legislation,

and represent a serious health public problem due to their mutagenic, carcinogenic and teratogenic effects [1,2]. Common *in vitro* toxicity evaluation methods such as the MTT assay, release of the enzyme lactate dehydrogenase assay, neutral red assay, and flow cytometry experiment are time-consuming, costly and difficult for long-term monitoring [3-6]. Therefore, it is critical to develop simple, low-cost, and sensitive toxicity detection method.

Cell-based electrochemical biosensors have emerged in last decade as a sensitive and noninvasive technique [7-9]. An *in-situ* electrochemical method was developed to integrate cell culture pretreatment with detection in the same cell culture dish [10]. The electrochemical behaviors of human breast cancer (MCF-7) and human cervical carcinoma (HeLa) cells based on graphene or carbon nanotubes modified glass carbon electrode were investigated [11,12]. However, due to the limitations of the size and sensitivity of the electrodes, this method can be only used for the detection of cells cultured in 60-mm or 100-mm dish with high amounts of cells. Moreover, only one or two completely overlapped signals were obtained, due to the similarity of intracellular electroactive species. To lower the need of high cell numbers and achieve high-throughput application, the vessel for cell culture and detection could be miniaturized to 96-well plate (diameter: 6.94 mm). Furthermore, if the electrode is sensitive enough to separate the mixture signals, it will be beneficial for elucidating cell physiology and *in vitro* toxicity of pollutants. Therefore, a miniaturized modified electrode with high sensitivity and selectivity is highly desirable.

Graphene oxide quantum dots (GOQDs) has gained high attention among

graphene-related materials. As zero-dimensional stable materials converted from two-dimensional graphene oxide sheets, GOQDs exhibit extraordinary properties owing to the edge and quantum confinement effects [13]. GOQDs hold great promise for sensor fabrication based on their distinct features of chemical inertness, ease of production, low-toxicity, and excellent biocompatibility [14,15]. The abundant hydroxyl and carboxylic groups render GOQDs hydrophilic and highly dispersible in water [16]. However, these oxygen-containing groups could hinder the motion of the electrolyte among the GOQDs, which limit their signal amplification and sensitivity [17]. On the other hand, the carbon nanotubes (CNTs) have been used for the development of electrochemical sensors due to their unique geometrical, mechanical and electronic properties [18,19]. Their surface can be activated with chemical treatments to achieve hydrophilic functional groups including carboxyl and hydroxyl. With high adsorption capacity, good electrical conductivity, and excellent surface-volume ratio, the functionalized CNTs are excellent supporting materials for surface modification of electrodes [20]. Given the similar structure and physical properties between GOQDs and CNTs, the hybridization could be formed via π-π interaction.

Furthermore, pencil graphite electrode (PGE) having smaller size (diameter: 0.7 mm) has been selected to minimize the size of the detection system. Compared with the traditional glass carbon electrode, PGE is advantageous regarding the wide potential window, low cost, disposability, good mechanical rigidity, and ease of

modification [21]. More importantly, PGE can eliminate the surface passivation problems, and have been used in various electroanalytical applications [22,23].

In the present work, a facile and green approach was developed for the graphene oxide quantum dots/carboxylated multi-walled carbon nanotubes (GOQDs/CMWCNTs) hybrid material, and modified with PGE to enhance sensitivity and selectivity. The modified working electrode, Pt wire (as the counter electrode) and Ag/AgCl (Sat'd) (as the pseudo-reference electrode) were integrated to assemble a miniaturized electrochemical sensor, which can be used for detection of cells cultured in 96-well plates. The usage of samples is saved from 1 mL in the traditional dish to 100 μL. Human hepatoma (HepG2) cells that have been proved as the stable and sensitive organisms for environmental toxicology were used as the model substrate for electrochemical detection [24-26]. There were four tasks in this study. First, GOQDs/CMWCNTs/PGE was developed and characterized. Second, the biochemical mechanism of the electrochemical behaviors of HepG2 cells was proposed. Third, the cell-based electrochemical biosensor was used for cytotoxicity evaluation of heavy metals including Cd, Hg and Pb, and phenols including 2,4-dinitrophenol (2,4-DNP), 2,4,6-trichlorophenol (2,4,6-TCP) and pentachlorophenol (PCP) (Scheme S1). Fourth, the MTT assay was adapted to compare with the electrochemical biosensor. This study provides a miniaturized platform which is available for the high-throughput application and a new insight into risk assessment of environmental pollutants from multiple perspectives.

2. Experimental

2.1. Reagents and solutions

MWCNTs (> 95%, 8-15 diameters and 0.5-2 μm lengths) were attained from Nanjing XFNANO Materials TECH Co., Ltd, China. Trypsin, purine bases 3-(4,5-dimethylthiazol-2-yl)-2,5-diphenyltetrazolium bromide (MTT), and dimethyl formamide (DMF) were purchased from Sigma (USA). $CdCl_2$, $HgCl_2$, $Pb(NO_3)_2$, 2,4-DNP, 2,4,6-TCP, PCP, sulfuric acid (H_2SO_4), hydrochloric acid (HCl) and other analytical reagents were obtained from J&K. Phosphate buffer saline (PBS) was prepared by 0.1 M Na_2HPO_4 and 0.1 M KH_2PO_4, and 0.1 M HCl or NaOH solution were added to adjust its pH to 7.4 [10], which was consistent with the normal extracellular pH value of human cells (7.4 ± 0.1). The stock standard solutions were prepared in the culture medium to concentrations of 1, 5, 10, 20, 40 μM for Cd and Hg, 10, 20, 40, 100, 150 μM for Pb, 100, 200, 400, 800, 1200 μM for 2,4,-DNP, 50, 100, 200, 300, 400 μM for 2,4,6-TCP, and 20, 40, 80, 100, 200 μM for PCP, respectively.

2.2. Apparatus

Electrochemical experiments were performed with a CHI 760E electrochemical workstation (Shanghai CH Instruments, China). The pH measurements were carried out on a PB-10 pH-meter (Sartorius, Germany). The micrographs were obtained using a JEOL 6340F Scanning Electron Microscope (SEM). The X-ray diffraction (XRD) patterns were detected on a Japan Rigaku D/max 2000 X-ray diffractometer equipped

with graphite monochromatized Cu Kα radiation (λ = 0.154 nm). Raman scattering spectra were recorded on a Jobin-Yvon HR 800 microscopic confocal Raman spectrometer with an Ar^+ laser source of 488 nm wavelength.

2.3. Cell Culture and Collection

The HepG2 cells were purchased from the COBIOER Biosciences Co., Ltd., Nanjing, China. The cells were cultured in Minimum Essential Medium (MEM) supplemented with 10% fetal bovine serum (FBS), 100 units mL^{-1} penicillin/streptomycin, 1% non-essential amino acids, and 1% sodium pyruvate in a humidified atmosphere with 5% CO_2 at 37 °C. Before pollutant exposure, the growth medium was discarded and replaced with the medium containing different concentrations of phenols or heavy metals. The heat inactivation and *in-situ* cell collection method developed by our group [10] were applied in this study. Briefly, the medium was removed from the culture plates, and PBS was added. The solution was heated in a water bath of 50 °C for 0.5 h to prepare the HepG2 cell suspension.

2.4. Synthesis of the GOQDs/CMWCNTs

The GOQDs was synthesized with the hydrothermal method [27]. Firstly, graphene oxide (GO) was prepared according to the Hummers method with a slight modification [28,29]. Then GO was treated at 250 °C for two hours in a tube furnace with a heating rate of 5 °C min^{-1} in the nitrogen atmosphere. 0.05 g graphene sheets were treated in the mixture containing 10 mL H_2SO_4 and 30 mL HNO_3 for 20 h under

mild ultrasonication. The oxidized graphene sheets were diluted and purified with the microporous membrane, and then redispersed in water. Then the suspension was heated in the autoclave at 200 °C for 5 h. The colloidal solution was dialyzed in the dialysis bag for 12 h to remove larger nanoparticles. 5.0 mg obtained GOQDs was dispersed in 10 mL double-distilled water under ultrasonic agitation for 5 h.

The CMWCNTs were prepared with the method reported in the literature [30] with little modification. In brief, the MWCNTs were refluxed with H_2SO_4/HNO_3 (3:1, v/v) at 120 °C for two hours to obtain CMWCNTs, and then washed with distilled water and dried at 60 °C. 5.0 mg purified CMWCNTs was then dispersed with 10 mL N,N-Dimethylformamide (DMF) by ultrasonic agitation.

10 mL 0.5 mg mL^{-1} GOQDs solution was added drop by drop into 10 mL 0.5 mg mL^{-1} CMWCNTs solution under vigorous stirring. The unbound GOQDs were removed by successive centrifugation (5000 rpm) and the suspension was washed with double distilled water and dried at 80 °C for ten hours. Finally, the obtained GOQDs/CMWCNTs were dispersed DMF with a final concentration of 0.5 mg mL^{-1} for use.

2.5. Fabrication of the GOQDs/CMWCNTs/PGE

After the pencil lead (T 0.7; length, 60 mm; Chenguang, China) had been wrapped by metallic wire to the end, an empty ballpoint pen refill was cut and used as the holder. The three electrodes were put through from a foam plastic insulation, which can keep them on the plates firmly. Before the modification, the PGE was firstly

treated in pH 6.0 PBS at the potential of +1.40 V for 60 s. This pretreatment was applied to remove any contaminant present on the surface and to improve the sensitivity [31,32]. 2.0 μL GOQDs/CMWCNTs solution was drop casted on the PGE surface to obtain the GOQDs/CMWCNTs/PGE through solvent evaporation. After each measurement, the GOQDs/CMWCNTs/PGE was renewed by scanning between 0.0 and +1.1 V in PBS (pH = 7.4) for five cycles. The obtained voltammograms exhibited comparable height and shape in the same sample solution with cyclic scan. After fifteen voltammetric measurements of the same cell sample, no obvious change was observed in both background current and peak current with relative standard deviation (RSD) < 5%.

2.6. MTT assay

The HepG2 cells (1.5×10^4 cells/well) were seeded in 96-well tissue culture plates (Sigma) and allowed to adhere at 37 °C. After 24 h of pre-incubation, either medium alone or medium containing phenol or heavy metal with different concentrations were added. After 24 h treatment, 20 μL 5 mg mL^{-1} MTT was added, and the cells were further incubated at 37 °C for four hours. The medium was then removed, and the formazan crystals were dissolved in DMSO. The measures were registered on an ELX800 Microplate Reader (BioTek Instruments, Inc., USA) and determined by absorbance values at 490 nm.

2.7. High-performance liquid chromatography (HPLC) measurements

HepG2 cell suspension was first treated at 50 °C for 30 min to remove the proteins. It was then filtrated through a 0.22 μm filter after the centrifugation at 10000 rpm for 30 min. The HPLC measurement was carried out using the Agilent 1100 Series HPLC pump (Agilent Technologies, Waldbronn, Germany) with an Ascentis RP-Amide column (4.0 × 250 mm) and a Diode Array Detector. The flow rate of the mobile phase (pH 4.0 KH_2PO_4) was set at 1.0 mL min^{-1}, and the injection volume was 20 μL.

2.8. Statistical analysis

The statistical analyses were conducted with SPSS 19.0 (SPSS Inc., USA) and Origin 8.0. In the figures, the dots represent the mean of three replicates, the error bars stand for the relative standard deviation (RSD, %) of three determinations. The probability value of $p < 0.05$ was set as the level for statistical significance.

3. Results and discussion

3.1. Characterization of the GOQDs/CMWCNTs composite

The surface morphology of each layer of the GOQDs/CMWCNTs composite showed the randomly oriented CMWCNTs with interconnected tubular structures (Fig. 1A), which was the characteristic feature of multi-walled carbon nanotubes [33]. As shown in Fig. 1B, most of GOQDs were uniformly dispersed with diameters of around 15 nm, which could be calculated according to the scale of SEM image under the amplifying model or by using the Image-Pro Plus software. The GOQDs/CMWCNTs surface indicated the uniform wrap of CMWCNTs with GOQDs

and this hybrid film exhibited high surface area (Fig. 1C). The structure of the highly conjugated GOQDs/CMWCNTs could prevent the aggregation of GOQDs and CMWCNTs, and facilitate the capture of pollutants. Moreover, the synthesized GOQDs/CMWCNTs hybrids were stable, uniform and well dispersed in water, indicating the simple and efficient synthesis process.

Fig. 1

Raman spectroscopy was employed to investigate the structures of GOQDs, CMWCNTs, and GOQDs/CMWCNTs (Fig. 2A). The spectra exhibit two remarkable peaks at ~ 1350 cm^{-1} and ~ 1580 cm^{-1} corresponding to D band and G band, respectively. The former is assigned to local defects and partially disordered structures of the sp^2 domains. The latter attributed to the E_{2g} phonon of sp^2 bonds of carbon atoms can be applied to evaluate the degree of graphitization [34]. The intensity ratio of D band to G band (I_D/I_G) is a useful value to estimate the amount of defect and disorder [35]. The GOQDs present the typical Raman signals of GOQDs with the I_D/I_G ratio of about 0.88 [36]. In the case of GOQDs/CMWCNTs, I_D/I_G value was 0.82, higher than that of CMWCNTs (0.72), indicating the increase in disorder after the introduction of high-quality GOQDs into CMWCNTs with the efficient π-π interaction.

The typical XRD profiles for GOQDs/CMWCNTs composite were compared with GOQDs and CMWCNTs (Fig. 2B). The GOQDs exhibited a peak centered at around 24.6° (002). The interlayer spacing is 0.39 nm, which is broader than that of graphite (0.34 nm) [37]. This was attributed to the presence of oxygenated functional groups,

which increased the d-space between graphene sheets. The CMWCNTs showed an intensive peak at 24.5° (002) and a minor peak at 42.5° (100), which originated from the graphite of sample [38]. GOQDs/CMWCNTs composite displayed a broad peak at 24.3° and a weak peak at 42.8°, demonstrating the successful formation of the hybrid during the preparation process.

Fig. 2

Electrochemical impedance spectroscopy (EIS) is a helpful technique to characterize the impedance changes of the electrode interface. In a typical impedance spectrum, the semicircular portion part at higher frequencies implies the electron transfer limited process and the diameter corresponds to the electron transfer resistance (R_{ct}) [39]. Compared with bare PGE, the R_{ct} of GOQDs/PGE increased dramatically due to the insulating nature of GOQDs, corresponding to the oxide group obtained from the oxidation process (Fig. 3). This phenomenon also demonstrated the repulsive electrostatic interactions between GOQDs and $[Fe(CN)_6]^{3-/4-}$ anions [40]. The R_{ct} value of CMWCNTs/PGE decreased compared to GOQDs/PGE and bare PGE, indicating the facile electron transfer reaction on CMWCNTs. For GOQDs/CMWCNTs/PGE composite, the R_{et} was far less than that of GOQDs/PGE, which proved that the CMWCNTs could act as an excellent electrochemical platform for electron transfer between GOQDs and PGE.

Fig. 3

3.2. Voltammetric behavior of HepG2 cell suspension

The cyclic voltammograms of HepG2 cell suspension at different electrodes showed that there was no peak at the bare PGE in HepG2 cell suspension (Fig. 4, curve a), while an oxidation peak appeared broadly at around +0.80 V at GOQDs/PGE (Fig. 4, curve b), and it was too small to distinguish. In case of CMWCNTs/PGE, two peaks at +0.67 V and +0.96 V appeared (Fig. 4, curve c). On GOQDs/CMWCNTs/PGE, three well-defined anodic peaks were observed at +0.67, +0.94 and +1.00 V (Fig. 4, curve d) ascribed to G/X, A and HX, respectively (the insert figure of Fig. 4). The oxidation currents were larger than other electrodes. Additionally, the GOQDs/CMWCNTs/PGE was compared with electrodes modified with graphene (erGO) and multi-walled carbon nanotubes (MWCNTs) (Fig. S1), which were the most commonly used nanomaterials in previous study [10-12]. Only two mixture signals were detected by the erGO/PGE and MWCNTs/PGE, attributed to guanine/xanthine and adenine/hypoxanthine, respectively. In contrast, the GOQDs/CMWCNTs/PGE was sensitive enough to separate the mixture signal of adenine/hypoxanthine, whose structures are very similar. Moreover, the peak current of guanine/xanthine at the GOQDs/CMWCNTs/PGE was 1.73 and 1.85 times as great as erGO/PGE and MWCNTs/PGE, respectively. The linear detection ranges of GOQDs/CMWCNTs/PGE are 0.2 to 180.0 μM for guanine, 0.2 to 150.0 μM for xanthine, 0.5 to 200.0 μM for adenine, 0.5 to 180.0 μM for hypoxanthine, and 2.5×10^3 to 6.0×10^6 cells mL^{-1} for HepG2 cells, respectively. The detection limits of GOQDs/CMWCNTs/PGE toward purine bases and HepG2 cells were also lower than those of the other electrodes (Table S1). The above results implied that the

GOQDs/CMWCNTs film had an excellent electrocatalytic activity towards the oxidation of purine bases, which might be caused by three reasons. First, the CMWCNTs can serve as conducting wires to promote charge transfer in electrochemical reactions [41,42], so that the intercalation of CMWCNTs can essentially roll GOQDs. The GOQDs/CMWCNTs nanohybrid can not only prevent the restacking of GOQDs but also exhibits larger surface area which is beneficial for enhancing the redox conversion. Second, the GOQDs/CMWCNTs hybrid possessed numerous functional groups, excellent conductivity, π-π bond, conducing to the conjugation between purine molecules and the electrode surface. Third, the synergistic effect between GOQDs and CMWCNTs potentially helped in facilitating the electron transfer. However, the peak current reduced rapidly from the second scan owing to the blocking effects of oxidation products (Fig. S2). Therefore, the first scan was applied in this study, and no corresponding reduction peak was observed in the inverse scan, indicating the irreversible electrode process.

Fig. 4

HPLC was used to confirm the existence of four purines in HepG2 cells. As shown in Fig. 5, the chromatographic peak of guanine (G), xanthine (X), adenine (A), and hypoxanthine (HX) appeared at 9.68, 10.71, 11.81 and 16.48 min, respectively. Four chromatographic peaks at 9.69, 10.73, 11.82, and 16.52 min of the HepG2 cell suspension were consisted with those of the purine bases mixture, which indicated the existence of G, X, A, and HX in HepG2 cell suspension. These intracellular purine bases could be concerned with the catabolism of guanosine monophosphate (GMP),

xanthosine monophosphate (XMP), adenosine monophosphate (AMP) and inosine monophosphate (IMP) as illustrated in Fig. 6. Nucleotidase can catalyze the conversion of GMP, XMP, AMP and IMP to guanosine, xanthosine, adenosine, and inosine, which are further catabolized to G, X, A, and HX by purine nucleoside phosphorylase [43,44]. The high cell viability can prompt the self-renewal and lead to the increase in purine nucleotide catabolism levels. Hence, as the intermediates of the cellular purine nucleotide metabolism, G, X, A, and HX can be used to evaluate the cell viability.

Fig. 5

Fig. 6

3.3. Effect of purine accumulation on voltammetric response of HepG2 cell suspension

The peak current was also related to the amount of purines accumulated on the modified electrode. The influence of purine accumulation was investigated using the linear sweep voltammetry (Fig. 7). When the time changed from 0 to 360 s, the peak current showed a dramatic increase. As the time further increased from 360 s to 540 s, the peak current did not change appreciably, indicating the four purines at electrode reached saturation. Accordingly, 360 s was employed as the optimal accumulation time for the electrochemical detection.

Fig. 7

3.4. Cytotoxicity assessment of heavy metals and phenols on HepG2 cells

The toxicity on HepG2 cells induced by Cd, Hg, Pb, 2,4,-DNP, 2,4,6-TCP, and PCP was examined at different concentrations (Fig. 8). All these priority pollutants exhibited significant toxicity in a concentration-dependent manner. The cytotoxicity was linear to the logarithm concentration of heavy metal or phenols. The linear regression equations and correlation coefficients (r) were derived (Table 1). The 24 hr IC_{50} based on the electrochemical signal I, signal II and signal III were 6.25, 5.62 and 7.99 μM for Cd, 9.65, 8.80 and 9.82 μM for Hg, and 47.95, 44.18 and 60.69 μM for Pb, respectively. Cd and Hg showed higher cytotoxicity, while Pb had a lower cytotoxic impact, which was in agreement with the results previously reported [45]. As persistent toxic metals, Cd, Hg, and Pb exerted cytotoxic action on HepG2 cells mainly via generating free radicals and inducing oxidative and nitrosative stress with depletion of antioxidants [46]. Three electrochemical signals related to the physiological change of cells declined due to the decrease in cell viability.

Compared with above heavy metals, the nitrophenol and chlorophenols exhibited relatively low toxicity on HepG2 cells. The IC_{50} calculated from three signals were 446.07, 418.21, 487.87 μM for 2,4-DNP, 195.89, 178.65 and 202.21 μM for 2,4,6-TCP, and 68.87, 61.24 and 78.71 μM for PCP, respectively. PCP is significantly the most toxic with the lowest IC_{50}, and 2,4-DNP is the least toxic with the highest IC_{50}. These results also confirmed that chlorine substitution was responsible for cytotoxicity of chlorophenols [47]. The cytotoxicity difference of three phenols on HepG2 cells may be attributed to their different metabolic mechanisms. PCP can

uncouple oxidative phosphorylation and lead to mitochondrial membrane damage, which is capable of inducing oxidative damage to DNA in cells [48,49]. Therefore, the metabolite of PCP may play a central role in PCP-induced highest cytotoxicity compared to 2,4-DNP and 2,4,6-TCP.

Moreover, the IC_{50} values obtained of heavy metals and phenols by the different signals are signal II < signal I < signal III, which may reflect that these priority pollutants have greater impacts on A than those on X/G and HX. It also reflects the toxicity differences of heavy metals and phenols on intracellular purine metabolism, which has significance for the study of the cellular physiological process. Therefore, compared with the electrochemical method based on one or two signal, the novel electrochemical biosensor can comprehensively assess the toxic effect of environmental pollutants from multiple perspectives.

Based on the data using the *in vitro* MTT assay, the IC_{50} are 10.23, 15.13, 76.56, 550.93, 239.83, and 79.87 μM for Cd, Hg, Pb, 2,4-DNP, 2,4,6-TCP, and PCP, respectively. The rank order of cytotoxic tendencies is Cd > Hg > Pb > PCP > 2,4,6-TCP > 2,4-DNP, which agreed with those by the cell-based electrochemical sensor. However, the IC_{50} values obtained by the electrochemical method are lower than those of the MTT assay, demonstrating that the former is more sensitive than the latter. The difference between the two techniques might be attributed to the difference in biochemical mechanism. MTT assay is based on the respiratory activity of the mitochondria, in which MTT is reduced in cells, forming formazan crystals that are then dissolved in dimethylsulfoxide [50]. Cell viability is determined based on the

optical density of dissolved crystals. However, this method has some disadvantages: sensitivity to multiple factors, poor linearity with cell number, and the dependence of cell metabolism on formazan [51]. In contrast, the electrochemical biosensor is rapid and label-free without adding any color developing agent, and directly detects the signals related to the nucleotide catabolism in cells, so that it is more accurate to assess the cytotoxicity. Moreover, this biosensor is lower cost compared with other purine metabolism-based electrochemical sensors [11,12]. In addition, the GOQDs/CMWCNTs/PGE is more sensitive due to the higher electrocatalytic activity [52], thus provides more exact information for research of physiological process of cells and toxicity effects of hazardous pollutants. By combining with the robotic technology developed in recent years [53], the proposed sensor also makes it possible for high-throughput analysis.

Fig. 8

Table 1

4. Conclusion

An integrated cell-based biosensor fabricated using the sensitive GOQDs/CMWCNTs composite was developed in this study, which was adaptable to 96-well plates instead of traditional cell culture dishes, and provided a utility cell viability evaluation platform. The correlation between electrochemical behaviors and nucleotide catabolism of HepG2 cells was established in a label-free way. Cytotoxicity of six priority pollutants was successfully evaluated via the changes of

three electrochemical signals derived from nucleotide catabolism of cells. The cytotoxic tendencies obtained by electrochemical signals were consisted with those of the traditional MTT assay. But the integrated cell-based biosensor exhibited higher sensitivity with lower IC_{50} values than the MTT assay. This cell-based electrochemical toxicity biosensor could be used for the *in situ* evaluation of environmental toxins and has potential for high-throughput detection of hazardous pollutants.

Acknowledgments

This research work was financially supported by the National Major Scientific and Technological Special Project of China (2014ZX07201-011-008), the National Natural Science Foundation of China (51178092, 51478097 and 51238001), the Fundamental Research Funds for the Central Universities (14ZZ1517) of China, and the State Scholarship Fund of China Scholarship Council.

References

[1] United States Environmental Protection Agency (USEPA), National recommended water quality criteria-correction, EPA 822-Z-99-001, 1999.

[2] United States Environmental Protection Agency (USEPA), Priority Pollutants. http://water.epa.gov/scitech/methods/cwa/pollutants.cfm/, 2015.

[3] S.M. Bryce, J.C. Bemis, S.L. Avlasevich, S.D. Dertinger, In vitro micronucleus

assay scored by flow cytometry provides a comprehensive evaluation of cytogenetic damage and cytotoxicity, Mutat. Res.-Gen. Tox. En. 630 (2007) 78-91.

[4] N.M. Franklin, J.L. Stauber, R.P. Lim, Development of flow cytometry-based algal bioassays for assessing toxicity of copper in natural waters, Environ. Toxicol. Chem. 20 (2001) 160-170.

[5] A.A. Stepanenko, V.V. Dmitrenko, Pitfalls of the MTT assay: direct and off-target effects of inhibitors can result in over/underestimation of cell viability, Gene 574 (2015) 193-203.

[6] X. Wang, P. Zhu, F. Pi, H. Jiang, J. Shao, Y. Zhang, X. Sun, A Sensitive and simple macrophage-based electrochemical biosensor for evaluating lipopolysaccharide cytotoxicity of pathogenic bacteria, Biosens. Bioelectron. 81 (2016) 349-357.

[7] H. Ben-Yoav, R.O. Almog, Y. Sverdlov, M. Sternheim, S. Belkin, A. Freeman, Y. Shacham-Diamand, Modified working electrodes for electrochemical whole-cell microchips, Electrochim. Acta 82 (2012) 109-114.

[8] W. Cheng, L. Ding, J. Lei, S. Ding, H. Ju, Effective cell capture with tetrapeptide-functionalized carbon nanotubes and dual signal amplification for cytosensing and evaluation of cell surface carbohydrate, Anal. Chem. 80 (2008) 3867-3872.

[9] L. Ding, D. Du, X. Zhang, H. Ju, Trends in cell-based electrochemical biosensors, Curr. Med. Chem. 15 (2008) 3160-3170.

[10] H. Qin, Q. Gao, H. Niu, Z. Wang, X. Zhu, J. Li, X. Yuan, D. Wu, An in situ

electrochemical detection method of cell viability, Analyst 138 (2013) 3372-3375.

[11] J. Li, J. Song, S. Bi, S. Zhou, J. Cui, J. Liu, D. Wu, Electrochemical estrogen screen method based on the electrochemical behavior of MCF-7 cells, J. Hazard. Mater. 313 (2016) 238-243.

[12] X. Zhu, H. Qin, J. Liu, Z. Zhang, Y. Lu, X. Yuan, D. Wu, A novel electrochemical method to evaluate the cytotoxicity of heavy metals, J. Hazard. Mater. 271 (2014) 210-219.

[13] P. Li, F. Di Stasio, G. Eda, O. Fenwick, S.O. McDonnell, H.L. Anderson, M. Chhowalla, F. Cacialli, Luminescent Properties of a water-soluble conjugated polymer incorporating graphene-oxide quantum dots, ChemPhysChem 16 (2015) 1258-1262.

[14] M. Favaro, F. Carraro, M. Cattelan, L. Colazzo, C. Durante, M. Sambi, A. Gennaro, S. Agnoli, G. Granozzi, Multiple doping of graphene oxide foams and quantum dots: new switchable systems for oxygen reduction and water remediation, J. Mater. Chem. A 3 (2015) 14334-14347.

[15] H. Sun, L. Wu, W. Wei, X. Qu, Recent advances in graphene quantum dots for sensing, Mater. Today 16 (2013) 433-442

[16] H. Pei, S. Zhu, M. Yang, R. Kong, Y. Zheng, F. Qu, Graphene oxide quantum dots@silver core-shell nanocrystals as turn-on fluorescent nanoprobe for ultrasensitive detection of prostate specific antigen, Biosens. Bioelectron. 74 (2015) 909-914.

[17] M. Mazloum-Ardakani, R. Aghaei, M. Abdollahi-Alibeik, A. Moaddeli, Fabrication of modified glassy carbon electrode using graphene quantum dot, gold nanoparticles and 4-(((4-mercaptophenyl) imino) methyl) benzene-1, 2-diol by self-assembly method and investigation of their electrocatalytic activities, J. Electroanal. Chem. 738 (2015) 113-122.

[18] Y. Li, S. Feng, S. Li, Y. Zhang, Y. Zhong, A high effect polymer-free covalent layer by layer self-assemble carboxylated MWCNTs films modified GCE for the detection of paracetamol, Sensor. Actuat. B-Chem. 190 (2014) 999-1005

[19] A. Merkoçi, M. Pumera, X. Llopis, B. Pérez, M. del Valle, S. Alegret, New materials for electrochemical sensing VI: carbon nanotubes, TrAC-Trend. Anal. Chem. 24 (2005) 826-838.

[20] P. Yáñez-Sedeño, J.M. Pingarrón, J. Riu, F.X. Rius, Electrochemical sensing based on carbon nanotubes, Anal. Chem. 29 (2010) 939-953.

[21] A. Özcan, Y. Şahin, A novel approach for the selective determination of tryptophan in blood serum in the presence of tyrosine based on the electrochemical reduction of oxidation product of tryptophan formed in situ on graphite electrode, Biosens. Bioelectron. 31 (2012) 26-31.

[22] A.A. Ensafi, E. Heydari-Bafrooei, M. Amini, DNA-functionalized biosensor for riboflavin based electrochemical interaction on pretreated pencil graphite electrode, Biosens. Bioelectron. 31 (2012) 376-381.

[23] L. Özcan, Y. Şahin, H. Türk, Non-enzymatic glucose biosensor based on overoxidized polypyrrole nanofiber electrode modified with cobalt (II)

phthalocyanine tetrasulfonate, Biosens. Bioelectron. 24 (2008) 512-517.

[24] M. Huang, Y. Kang, W. Wang, C.Y. Chan, X. Wang, M.H. Wong, Potential cytotoxicity of water-soluble fraction of dust and particulate matters and relation to metal(loid)s based on three human cell lines, Chemosphere 135 (2015) 61-66.

[25] B. Novotnik, J. Ščančar, R. Milačič, M. Filipič, B. Žegura, Cytotoxic and genotoxic potential of Cr (VI), Cr (III)-nitrate and Cr (III)-EDTA complex in human hepatoma (HepG2) cells, Chemosphere 154 (2016) 124-131.

[26] L. Peng, M. He, B. Chen, Q. Wu, Z. Zhang, D. Pang, Y. Zhu, B. Hu, Cellular uptake, elimination and toxicity of CdSe/ZnS quantum dots in HepG2 cells, Biomaterials 34 (2013) 9545-9558.

[27] D. Pan, J. Zhang, Z. Li, M. Wu, Hydrothermal route for cutting graphene sheets into blue-luminescent graphene quantum dots, Adv. Mater. 22.6 (2010) 734-738.

[28] W.S. Hummers Jr, R.E. Offeman, Preparation of graphitic oxide, J. Am. Chem. Soc. 80 (1958) 1339-1339.

[29] Y. Xu, H. Bai, G. Lu, C. Li, G. Shi, Flexible graphene films via the filtration of water-soluble noncovalent functionalized graphene sheets, J. Am. Chem. Soc. 130 (2008) 5856-5857.

[30] S.W. Lee, B.S. Kim, S. Chen, Y. Shao-Horn, P.T. Hammond, Layer-by-layer assembly of all carbon nanotube ultrathin films for electrochemical applications, J. Am. Chem. Soc. 131 (2008) 671-679.

[31] A. Erdem, D.O. Ariksoysal, H. Karadeniz, P. Kara, A. Sengonul, A.A. Sayiner, M. Ozsoz, Electrochemical genomagnetic assay for the detection of hepatitis B virus

DNA in polymerase chain reaction amplicons by using disposable sensor technology, Electrochem. Commun. 7 (2005) 815-820.

[32] Ö. Sağlam, B. Kızılkaya, H. Uysal, Y. Dilgin, Biosensing of glucose in flow injection analysis system based on glucose oxidase-quantum dot modified pencil graphite electrode, Talanta 147 (2016) 315-321.

[33] M. AbduláAziz, Surfactant and polymer-free electrochemical micropatterning of carboxylated multi-walled carbon nanotubes on indium tin oxide electrodes, Chem. Commun. 7 (2008) 826-828.

[34] X.F. Zhang, Q. Xi, A graphene sheet as an efficient electron acceptor and conductor for photoinduced charge separation, Carbon 49 (2011) 3842-3850.

[35] G.H. Moon, Y. Park, W. Kim, W. Choi, Photochemical loading of metal nanoparticles on reduced graphene oxide sheets using phosphotungstate, Carbon 49 (2011) 3454-3462

[36] L. Zhang, Z.Y. Zhang, R.P. Liang, Y.H. Li, J.D. Qiu, Boron-doped graphene quantum dots for selective glucose sensing based on the “abnormal” aggregation-induced photoluminescence enhancement, Anal. Chem. 86 (2014) 4423-4430.

[37] Y. Sun, S. Wang, C. Li, P. Luo, L. Tao, Y. Wei, G. Shi, Large scale preparation of graphene quantum dots from graphite with tunable fluorescence properties, Phys. Chem. Chem. Phys. 15 (2013) 9907-9913.

[38] Y.K. Kim, H. Park, Light-harvesting multi-walled carbon nanotubes and CdS hybrids: application to photocatalytic hydrogen production from water, Energ.

Environ. Sci. 4 (2011) 685-694.

[39] I.I. Suni, Impedance methods for electrochemical sensors using nanomaterials, TrAC-Trend. Anal. Chem. 27 (2008) 604-611.

[40] H. Razmi, R. Mohammad-Rezaei, Graphene quantum dots as a new substrate for immobilization and direct electrochemistry of glucose oxidase: application to sensitive glucose determination, Biosens. Bioelectron. 41 (2013): 498-504.

[41] J.J. Gooding, R. Wibowo, J. Liu, W. Yang, D. Losic, S. Orbons, F.J. Mearns, J.G. Shapter, D.B. Hibbert, Protein electrochemistry using aligned carbon nanotube arrays, J. Am. Chem. Soc. 125 (2003) 9006-9007.

[42] P. Sharma, V. Bhalla, V. Dravid, G. Shekhawat, E.S. Prasad, C.R. Suri, Enhancing electrochemical detection on graphene oxide-CNT nanostructured electrodes using magneto-nanobioprobes, Sci. Rep.-UK 2 (2012) 877.

[43] W. Dudzinska, A.J. Hlynczak, E. Skotnicka, M. Suska, The purine metabolism of human erythrocytes, Biochemistry-Moscow 71 (2006) 467-475.

[44] A. Torrecilla, A.F. Marques, R.D. Buscalioni, J. Oliveira, N.A. Teixeira, E.A. Atencia, A. Sillero, Metabolic fate of AMP, IMP, GMP and XMP in the cytosol of rat brain: an experimental and theoretical analysis, J. Neurochem. 76 (2001) 1291-1307

[45] E. Egiebor, A. Tulu, N. Abou-Zeid, I.T. Aighewi, A. Ishaque, The kinetic signature of toxicity of four heavy metals and their mixtures on MCF7 breast cancer cell line, Inter. J. Env. Res. Pub. Heal. 10 (2013) 5209-5220.

[46] S.A. Saïdi, M.S. Azaza, P. Windmolders, J. van Pelt, A. El-Feki, Cytotoxicity

evaluation and antioxidant enzyme expression related to heavy metals found in tuna by-products meal: an in vitro study in human and rat liver cell lines, Exp. Toxicol. Pathol. 65 (2013) 1025-1033.

[47] F. Zhao, K. Mayura, R.W. Hutchinson, R.P. Lewis, R.C. Burghardt, T.D. Phillips, Developmental toxicity and structure-activity relationships of chlorophenols using human embryonic palatal mesenchymal cells, Toxicol. Lett. 78 (1995) 35-42.

[48] J. Chen, J. Jiang, F. Zhang, H. Yu, J. Zhang, Cytotoxic effects of environmentally relevant chlorophenols on L929 cells and their mechanisms, Cell Boil. Toxicol. 20 (2004) 183-196.

[49] C. Pietsch, J. Hollender, F. Dorusch, P. Burkhardt-Holm, Cytotoxic effects of pentachlorophenol (PCP) and its metabolite tetrachlorohydroquinone (TCHQ) on liver cells are modulated by antioxidants, Cell Biol. Toxicol. 30 (2014) 233-252.

[50] A.A. van de Loosdrecht, E. Nennie, G.J. Ossenkoppele, R.H. Beelen, M.M. Langenhuijsen, Cell mediated cytotoxicity against U 937 cells by human monocytes and macrophages in a modified colorimetric MTT assay: a methodological study, J. Immunol. Methods 141 (1991) 15-22.

[51] P. Marqués-Gallego, H. den Dulk, C. Backendorf, J. Brouwer, J. Reedijk, J.F. Burke, Accurate non-invasive image-based cytotoxicity assays for cultured cells, BMC Biotechnol. 10 (2010) 43.

[52] X. Guo, Q. Wang, J. Li, J. Cui, S. Zhou, S. Hao, D. Wu, A mini-electrochemical system integrated micropipet tip and pencil graphite electrode for detection of anticancer drug sensitivity in vitro, Biosens. Bioelectron. 64 (2015) 594-596.

[53] S. Theanponkrang, W. Suginta, H. Weingart, M. Winterhalter, A. Schulte, Robotic voltammetry with carbon nanotube-based sensors: a superb blend for convenient high-quality antimicrobial trace analysis, Int. J. Nanomed. 10 (2015) 859-868.

Figure captions

Fig. 1. SEM images of the CMWCNTs (A), GOQDs (B), and GOQDs/CMWCNTs (C).

Fig. 2. Raman spectra (A) and XRD patterns (B) of GOQDs, CMWCNTs, and GOQDs/CMWCNTs composite.

Fig. 3. EIS of different electrodes in 5.0 mM $[Fe(CN)_6]^{3-/4-}$ containing 0.1 M KCl with the frequencies swept from 0.1 Hz to 100 kHz.

Fig. 4. Cyclic voltammograms of HepG2 cell suspension at: (a) PGE, (b) GOQDs/PGE, (c) CMWCNTs/PGE, and (d) GOQDs/CMWCNTs/PGE, cell concentration: 5.0×10^5 cells mL^{-1}. Inset: Baseline-corrected linear sweep voltammograms of (a) HepG2 cell suspension, (b) 30.0 μM xanthine, (c) 40.0 μM guanine, (d) 30.0 μM adenine and (e) 30.0 μM hypoxanthine in pH 7.4 PBS at GOQDs/CMWCNTs/PGE. Cell concentration: 6.0×10^5 cells mL^{-1}.

Fig. 5. Chromatogram of purine mixture (a) and HepG2 cell eluents (b). Cell concentration: 3.0×10^6 cells mL^{-1}; purine concentration: 15.0 μg mL^{-1}.

Fig. 6. Intracellular purine nucleotide metabolism. NT: nucleotidase; PNP: purine nucleoside phosphorylase.

Fig. 7. Influence of accumulation time on the electrochemical signal I (a), signal II (b), and signal III (c) of HepG2 cells suspension in pH 7.4 PBS. Cell concentration: 6.0×10^5 cells mL^{-1}.

Fig. 8. Cytotoxicity of Cd, Hg, Pb, 2,4-DNP, 2,4,6-TCP and PCP on HepG2 cells detected by the electrochemical biosensor and the MTT assay.

Fig. 1

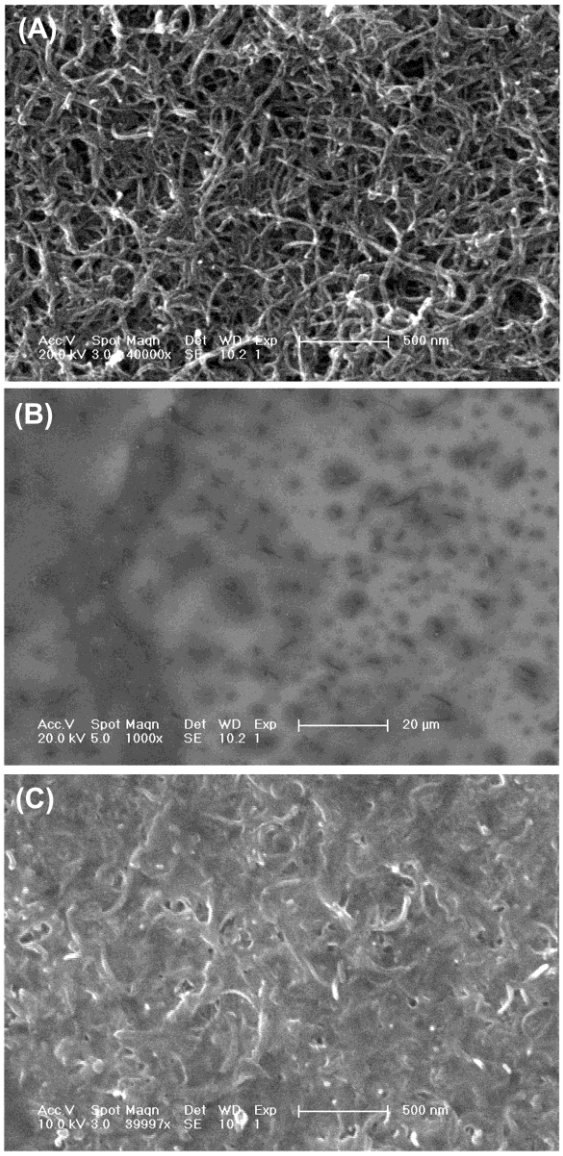

Fig. 2

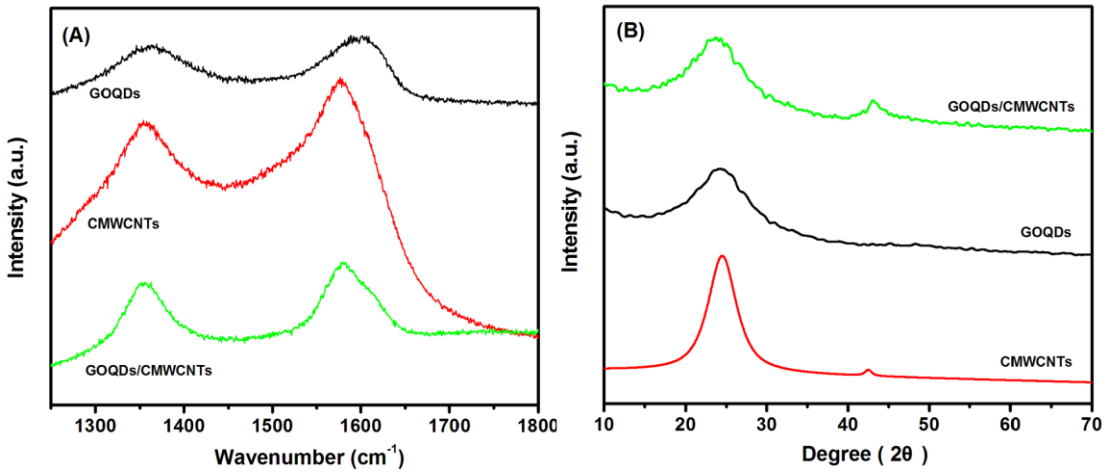

Fig. 3

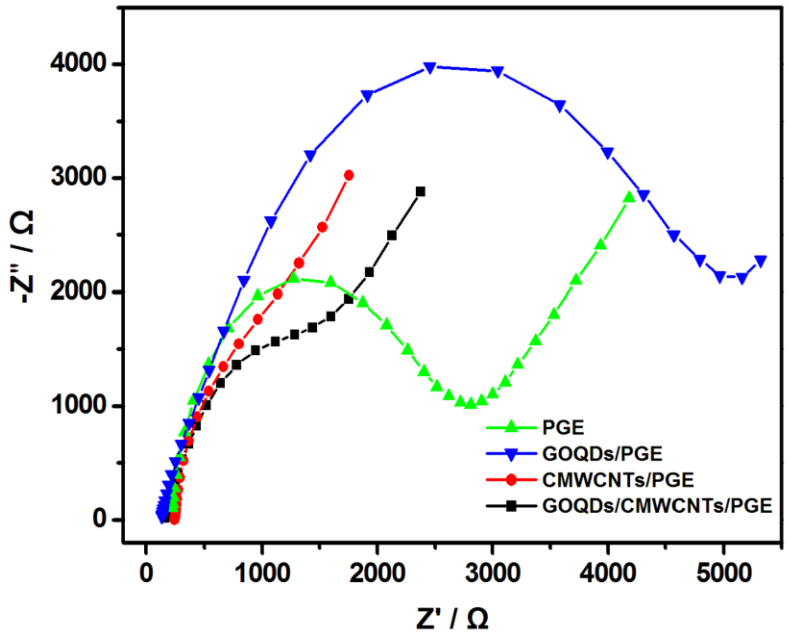

Fig. 4

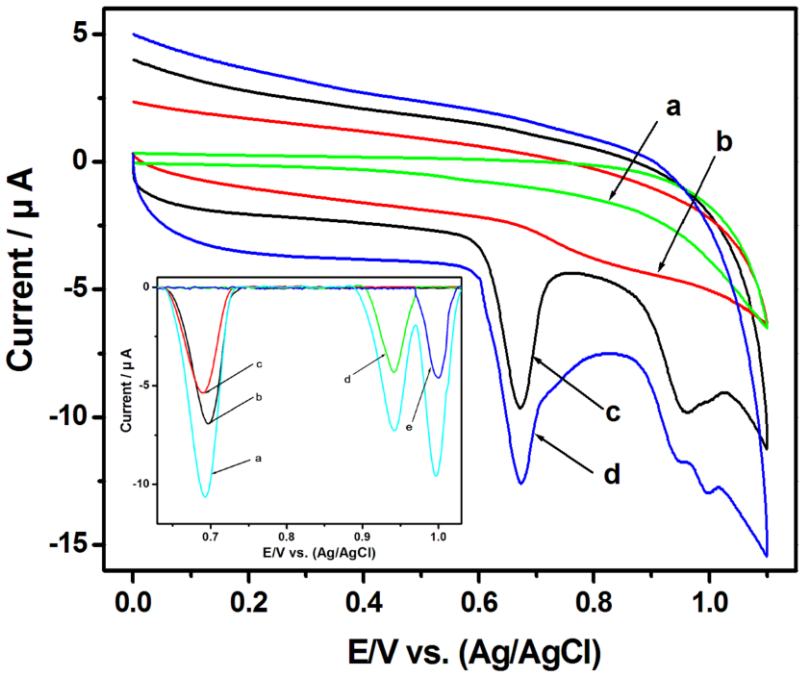

Fig. 5

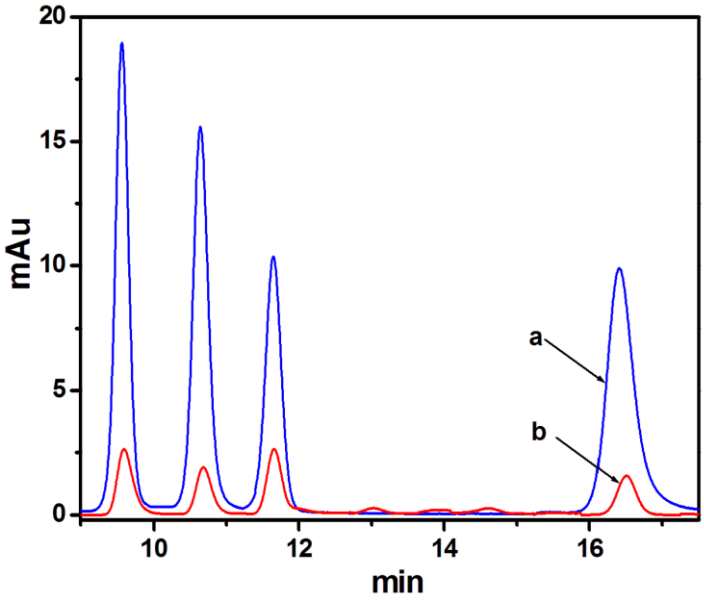

Fig. 6

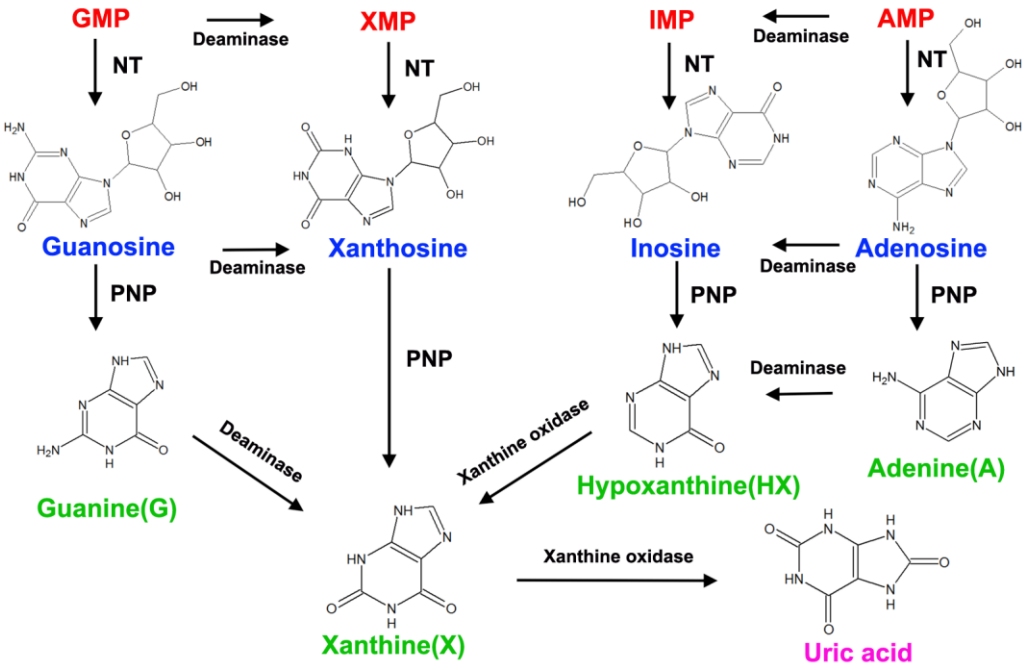

Fig. 7

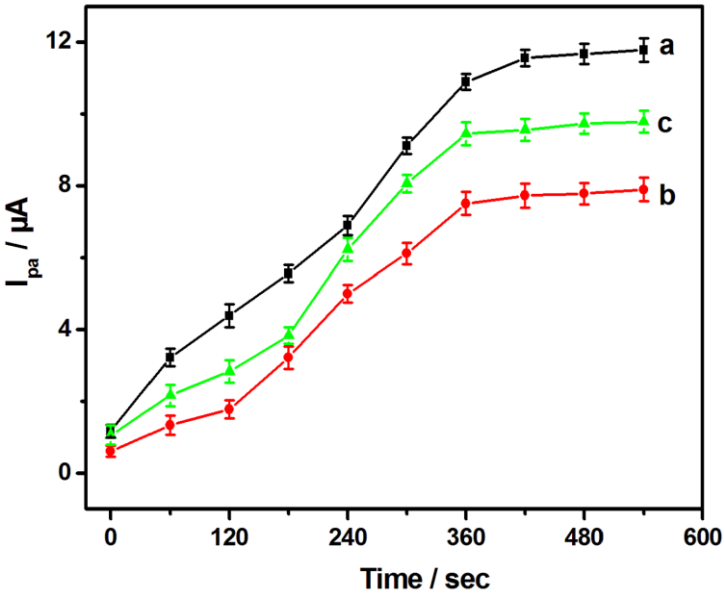

Fig. 8

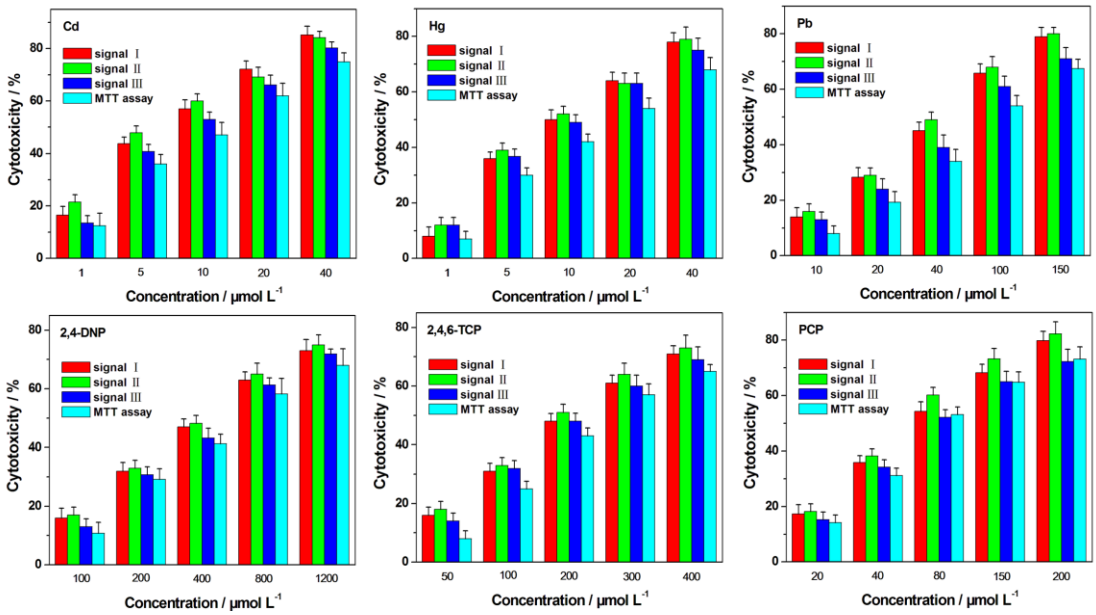

Table 1. The linear relationship between the concentration and cytotoxicity of heavy metals and phenols on HepG2 cells.

Toxicant	Signal I	Signal II	Signal III	MTT assay
Cd	$Y = 43.06\ X + 15.30$ (r = 0.9973)	$Y = 38.38\ X + 21.21$ (r = 0.9970)	$Y = 41.35\ X + 12.67$ (r = 0.9984)	$Y = 39.00\ X + 10.61$ （r = 0.9822)
Hg	$Y = 43.76\ X + 6.92$ (r = 0.9983)	$Y = 41.19\ X + 11.09$ (r = 0.9968)	$Y = 39.55\ X + 10.76$ (r = 0.9970)	$Y = 37.80\ X + 5.40$ (r = 0.9846)
Pb	$Y = 54.64\ X - 41.84$ (r = 0.9968）	$Y = 54.56\ X - 39.76$ (r = 0.9960)	$Y = 50.12\ X - 39.37$ (r = 0.9943)	$Y = 50.03\ X - 44.28$ (r = 0.9878)
2,4-DNP	$Y = 52.46\ X - 88.99$ (r = 0.9997)	$Y = 53.54\ X - 90.35$ (r = 0.9996)	$Y = 53.58\ X - 94.04$ (r = 0.9963)	$Y = 51.88\ X - 92.21$ (r = 0.9864)
2,4,6-TCP	$Y = 60.34\ X - 88.30$ (r = 0.9915)	$Y = 60.98\ X - 87.33$ (r = 0.9938)	$Y = 59.94\ X - 88.21$ (r = 0.9975)	$Y = 63.39\ X - 100.86$ (r = 0.9904)
PCP	$Y = 60.79\ X - 61.73$ (r = 0.9966)	$Y = 63.52\ X - 63.51$ (r = 0.9961)	$Y = 56.47\ X - 57.07$ (r = 0.9972)	$Y = 59.03\ X - 62.30$ (r = 0.9847)

Y and *X* stand for the cytotoxicity (percent inhibition) and logarithm of toxicant concentration, respectively.